

Communication

Triboelectrification-enabled thin-film tactile matrix for self-powered high-resolution imaging

Xiao Xiao Zhu^{a,c}, Ze Bin Li^{a,c}, Xiao Shi Li^g, Li Su^{a,c}, Xiao Yan Wei^{a,c}, Shuang Yang Kuang^{a,c}, Bing Wu Su^{a,c}, Jin Yang^g, Zhong Lin Wang^{a,c,e,f,*}, Guang Zhu^{a,b,c,d,e,*}

^a CAS Center for Excellence in Nanoscience, Beijing Key Laboratory of Micro-Nano Energy and Sensor, Beijing Institute of Nanoenergy and Nanosystems, Chinese Academy of Sciences, Beijing 100083, China

^b Department of Mechanical, Materials and Manufacturing Engineering, The University of Nottingham Ningbo China, Ningbo 315100, China

^c School of Nanoscience and Technology, University of Chinese Academy of Sciences, Beijing 100049, China

^d New Materials Institute, The University of Nottingham Ningbo China, Ningbo 315100, China

^e Center on Nanoenergy Research, School of Physical Science and Technology, Guangxi University, Nanning 530004, China

^f School of Materials Science and Engineering, Georgia Institute of Technology, Atlanta, GA 30332, USA

^g Department of Optoelectronic Engineering, Chongqing University, Chongqing 400044, China

ARTICLE INFO

Keywords:

Tactile sensor
Triboelectrification
Self-powered
Sensor matrix

ABSTRACT

Tactile sensors have broad applications in human-machine interfacing technologies. In this work, we report a type of a thin-film-based flexible integrated triboelectric sensing matrix (ITESM) that is of high resolution and large area. It has a total of 3600 sensing units and a resolution of 50 dots per inch (dpi), which are 14 times and 25 times of the state-of-the-art works on the triboelectric sensor array, respectively. When touched by an external object, the ITESM generates a voltage signal in its bit electrode lines and word electrode lines due to the combination of triboelectrification and electrostatic induction. With the assistance of a signal processing circuit that filters and amplifies the electric signal, an average voltage signal of 0.4 V can be acquired. Due to the design of a shielding layer, the electrostatic induction among adjacent electrode lines are effectively eliminated, resulting in a near end crosstalk (NEXT) of merely 0.05. As a result, single-point as well as multi-point contacts can be explicitly revealed. Therefore, the ITESM in this work presents a major step in the direction of high-resolution and large-area triboelectric sensing.

1. Introduction

Tactile sensors, which act as transducers transforming physical, chemical, biological and mechanical signals into electrical signals, are important means of human-machine interactions [1–4]. Although various types of tactile sensors based on different working principles have been reported [5–10], energy consumption is a universal problem that needs to be addressed [11–13]. Despite of low energy consumption of a single sensor unit [14–17], the amount of the energy consumed by an array of tactile units becomes considerable. Recently, triboelectric sensors based on the combination of triboelectrification and electrostatic induction have been extensively reported [18–20], which could generate electric signal by the conversion of ambient mechanical energy. These triboelectric sensors have exhibited high sensitivity, self-powered operation, and simple fabrication process. By arranging a number of triboelectric sensor units into an array, researchers have achieved recording the position, the trajectory, and the shape profile of

objects that are in contact with the sensor array [20,21,23–26]. There were usually two strategies in arranging the sensor units in an array [20,25]. One approach was that each and every sensor unit was individually wired [20]. Although it may benefit the signal-to-noise ratio, the number of wires may become overwhelming, which poses a significant challenge for data acquisition interface. As a result, large-area and high-resolution tactile sensing may not be realized. For the state-of-the-art research following this strategy, the size of a sensing unit was reported to be as small as 5 mm, while the total number of units was no more than 16×16 [25]. The other strategy was constructing electrodes that had a cross bar configuration. The interaction between a bit electrode line and a word electrode line is defined as a sensing unit, which largely reduces the number of wires [25]. However, cross talk among the electrode lines attributed to electrostatic induction compromises the area resolution of the triboelectric tactile sensor array. So far, the reported highly resolution was merely 2 dpi [25]. Therefore, it is highly desired to develop a type of triboelectric tactile sensor array that

* Corresponding authors at: Beijing Institute of Nanoenergy and Nanosystems, Chinese Academy of Sciences, Beijing 100083, China.
E-mail addresses: zlwang@binn.cas.cn (Z.L. Wang), zhuguang@binn.cas.cn (G. Zhu).

possesses both high density and large area.

In this work, we report a type of a thin-film-based flexible integrated triboelectric sensing matrix (ITESM) for high-resolution and self-powered imaging. Resorting to the means of micro- and nano-fabrication, multiple thin-film layers including bit electrode lines and word electrode lines are constructed onto a flexible substrate. When touched by an external object, triboelectrification coupled with electrostatic induction can give rise to a voltage signal at the corresponding bit electrode lines as well as word electrode lines. With the assistance of a signal processing circuit that filters and amplifies the generated electric signal, an average voltage signal of 0.4 V can be acquired. Owing to the design of a shielding layer, the electrostatic induction among adjacent electrode lines are effectively suppressed, resulting in a NEXT of merely 0.05. As a result, single-point as well as multi-point contacts can be explicitly revealed. The ITESM reported here has an overall thickness of 20 μm , which is the thinnest triboelectric sensor array reported by far [25]. It has an effective area of $3 \times 3 \text{ cm}^2$ that contains a total of 3600 sensing units, which is 14 times of the state-of-the-art works on the triboelectric sensor array [25]. The sensing resolution reaches 50 dpi, which again poses a 25-times enhancement over the published works [25]. The ITESM in this work presents a major step in the direction of high-resolution and large-area triboelectric sensing. It is expected to promote the potential practical applications of the triboelectric sensor in human-machine interfacing technologies such as electric signature, fingerprint recognition, artificial skin and security monitoring, etc.

2. Results and discussion

The schematic diagram of the ITESM is shown in Fig. 1a with 3600 sensing units in a sixty-by-sixty matrix. The ITESM contains the following components, including an upper electrification layer made of thermoplastic polyurethanes (TPU), a lower electrification layer made of dichloro[2,2]paracyclophane (Parylene-C), a bit electrode layer made of silver, an upper insulation layer made of Parylene-C, a shielding layer made of silver, a lower insulation layer made of Parylene-C and a word electrode layer made of silver. The layer-by-layer

structure is constructed on top of a thin-film substrate made of Polyimide (PI). They are stacked sequentially on substrate layer from the top to the bottom, as shown in Fig. 1a and b. A gap of 5 mm height is maintained between the two electrification layers. Once external objects touches the ITESM, the contact between the TPU and the Parylene-C actually occurs, which rules out the dependence of the electric signal on the materials of the contact objects. The bit electrode line, the word electrode line and the shielding layer are laid underneath the lower electrification layer in separate layers. The units with hollow squares are connected to form the bit electrode line, while the units with solid squares are lined up forming the word electrode line. The units between the two electrode layers have one-to-one correspondence. A shielding layer consisting of a hollow square array lies between the bit electrode layer and the word electrode layer. The size of the individual hollow squares in the shielding layer is smaller than that of the bit electrode line but equivalent to the solid squares of the word electrode line. This layer can effectively eliminate the electrostatic induction among the bit electrode lines and the word electrode lines in vertical direction as well as adjacent sensing units of the same electrode layer in lateral direction. Therefore, crosstalk will be largely reduced, which has been systematically justified in our previous work [26]. Two insulation layers composed of Parylene-C lie between the shielding layer and the electrode layers to prevent electric shorts. Fig. 1c shows the picture of the fabricated ITESM with an effective sensing area of $3 \times 3 \text{ cm}^2$. The enlarged view of the arrayed sensing units in an optical microscope image is exhibited in Fig. 1d, which shows that the two electrode layers are well stacked and aligned in the vertical direction. The size of a single unit is $500 \times 500 \mu\text{m}^2$, which indicates the ITESM has an area resolution of 50 dpi. This resolution is 25 times higher than recently reported triboelectric tactile sensor that had crossbar-shaped electrodes [25]. The overall thickness of the as-fabricated sixty-by-sixty sensing matrix is only 20 μm and can be easily bent as shown in Fig. 1e.

When contacted with the TPU membrane, the Parylene-C marked as the lower electrification layer will gain significant negative triboelectric charges due to the triboelectrification effect [22]. To improve the triboelectric charge density on the contacting surfaces, here two means

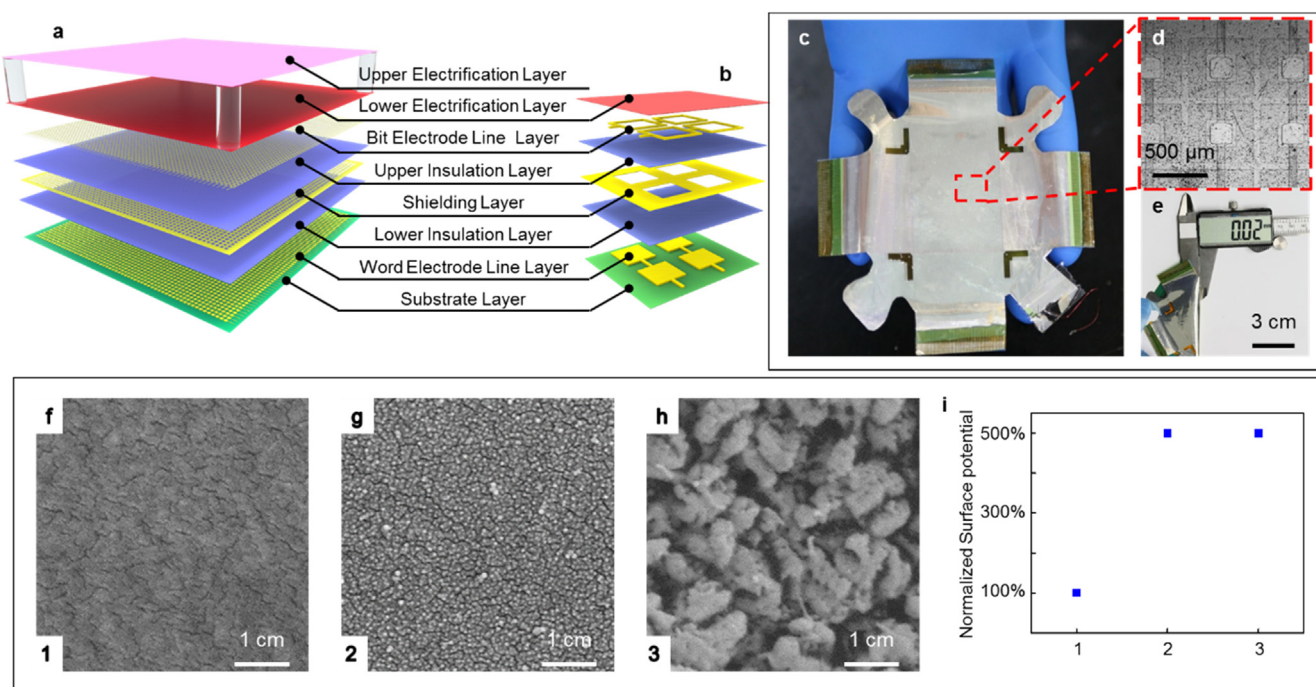


Fig. 1. Structural illustration and material characterizations of the ITESM. (a) Schematic diagram of the ITESM in a sixty-by-sixty array. (b) Break-down view of a 2×2 array. (c) Photograph of the ITESM and its enlarged view (d). (e) Illustration of the high flexibility of the ITESM. Surface morphology of the original (f), the nanoparticle-modified (g) and the ICP etched (h) lower electrification layer in SEM images and (i) normalized surface electric potential.

were used to modify the surface of the lower electrification layer, i.e. polytetrafluoroethylene (PTFE) nanoparticles deposition and induced couple plasma (ICP) etching. The surface morphologies of a plain surface, a nanoparticle-modified surface, and an ICP etched surface in scanning electron microscope (SEM) are shown in Fig. 1f–h, respectively. A surface electric potential meter is used to measure the surface electric potential of the lower electrification layer after repeatedly contacts with the TPU membrane. As Fig. 1i shown, after normalized calculation, the electric potential of the modified surface is improved by at least four times compared to the original plain surface. The surface electric potential is in great accordance to amplitude of the voltage signal, which benefits the data acquisition process. As a result, the means that can generate the highest surface potential, i.e. ICP etching, is adopted to modify the lower electrification layer.

The basic sensing principle of the ITESM is based on the combination of triboelectrification and electrostatic induction between the Parylene-C based lower electrification layer and the TPU-based upper electrification layer. When an object dynamically interacts with the ITESM, a voltage signal is produced on the electrode layers, which can be measured after being amplified by a signal processing circuit. The details of the signal processing circuit will be discussed later. To elaborate this process, a sketch of a cross-sectional viewed ITESM is drawn in Fig. 2a. As discussed above, when contacted with the TPU membrane, the Parylene-C material would gain electrons and become negatively charged, while the TPU membrane would lose the same amount of electrons and become positively charged. When the object is withdrawn, the TPU membrane would separate away from the Parylene-C. The triboelectric charges of opposite signs are maintained on both sides of the surface. Induced positive charges will be accumulated on the word electrode line and the bit electrode line beneath the contacted sensing unit. As a result of the repeated contacts and separations, the word electrode line and the bit electrode line would generate a cyclic voltage signal, which reaches ~ 0.4 V after being amplified, as shown in Fig. 2b. The signals from the word lines and the bit lines both show alternating behavior. The difference lies in the observation that the peaks from the word lines and the bit lines are not synchronized, as indicated by the arrows in Fig. 2b. This difference is explained as follows. The word line electrode and the bit line electrode have complementary patterns. For a single sensing unit, the word electrode line has a solid square pattern in the center, while the bit electrode line has a hollow square pattern along the circumference. In this work, a tip of a marker pen was used to excite the sensor. Made of elastic sponge, the marker tip can be squeezed when being pressed; and the contact area between the tip and the sensor becomes larger if higher pressure is exerted. When the marker tip is in initial contact with the sensor, the word electrode line is excited because the word line pattern sits at the center (the peak “1” in Fig. 2b). Then the signal from the bit line follows when the marker tip forms more tight contact with the sensor (the peak “2” in Fig. 2b). During the separating process, the situation is reserved. The marker tip firstly separates away from the bit line, generating the peak “3” in Fig. 2b. Finally, when the marker tip separates away from the center region of the sensing unit, the peak “4” is produced in Fig. 2b. The signal-generating process is illustrated in Fig. 2c to f in sequence. In general, the difference of the voltage signal from the two electrode layers is attributed to the deformable marker tip that has variable contact area with the sensor. The shielding layer has a uniform electric potential of 0 V and effectively suppresses the crosstalk between the sensing units. In other words, the word electrode line and the bit electrode line that are not actually touched will not produce undesirable voltage signal. As a result, the accurate contact position would be identified and revealed by recognizing the two-dimensional coordinates of the word electrode line and the bit electrode line that generate effective voltage signal, as shown in Fig. 2g.

The single-point experimental results of the electric measurement on the sixty-by-sixty ITESM are presented in Fig. 3. To verify the uniformity of the ITESM, the background signal from randomly selected 24

word electrode lines and 24 bit electrode lines is measured, as shown in Fig. 3a and b. According to the color bar reference, the maximum background signal is found to be no more than 2 mV when no contacts occur, which proves the high uniformity of the ITESM. The enlarged illustration of the word electrode line ($W_{39}\sim W_{48}$) and the bit electrode lines ($B_{39}\sim B_{48}$) clearly describes the very small fluctuation of the background signal, as shown in Fig. 3c and d, respectively. A single-point contact test was conducted at the position indexed as (W_{20}, B_{34}) corresponding to the intersection between the word electrode line W_{20} and the bit electrode line B_{34} . The measured voltage signal from the 48 selected electrode lines is presented in Fig. 3e and f. As discussed above, the accurate contact position could be identified by deducing the word electrode line and the bit electrode line in the two-dimensional coordinates of the sensor matrix. To clearly illustrate and compare the amplitude of the voltage signal acquired from all of the selected electrode lines, Fig. 3g and h present the measured data in a side view corresponding to Fig. 3e and f, respectively. Attributed to the screening effect from the shielding layer, the amplitude of the voltage signal reaches ~ 0.4 V from the word electrode line W_{20} as well as the bit electrode line B_{34} , while the maximum voltage signal from other electrode lines is only ~ 0.02 V. Here, NEXT is used to indicate the difficulty of signal recognition, which can be expressed as

$$NEXT = V_n/V_s \quad (1)$$

where V_s is the voltage signal from the sensing unit that is actually contacted, and V_n is the voltage signal from the nearest adjacent sensing unit [27]. The lower value of the NEXT is, the less crosstalk among the electrode lines is, and the easier the signal recognition becomes. Here, the voltage signal acquired from the electrodes W_{20} and B_{34} is 20 times higher than the other electrode lines. Therefore, the NEXT is calculated to be 0.05, which represents the readiness of signal recognition and supports the effectiveness of the shielding layer in suppressing the crosstalk among the electrode lines. To evaluate the stability of the ITESM, the sensing matrix was tested under repeated contacts at a frequency of 1 Hz. Ten cyclic contacts produce cycled patterns of the voltage signal in a peak wave, as presented in Fig. 3i and j. The amplitude of the voltage signal of the word electrode line and the bit electrode line underneath the contacted unit are repeatable at ~ 0.4 V, while the voltage signal from other electrode lines keeps lower than 0.02 V, which proves stability of the ITESM.

Because of the low crosstalk, the ITESM is used to reflect the shape profile of the contact object. Fig. 4 illustrates a prototype of a demonstration system. As shown in Fig. 4a, an experimental setup was built up for investigating the feasibility of an ITESM used in image sensing. A square contact object was affixed to a linear motor, which was directly above the central region of the ITESM, as shown in Fig. 4b. The produced voltage signal was processed by the signal processing circuit before being inputted into a multi-channel data acquisition system. Fig. 4c shows a schematic diagram of the signal processing flow. The optimized signal processing was specially designed to remove the interference from low-frequency noise in ambient environment for more precisely detecting the voltage signal. It consists of a signal processing part and a sampling part. The signal processing part processes the voltage signal mainly in two steps. Firstly, the acquired original voltage signal is filtered to remove environment noises such as power frequency interference and electromagnetic interference. Then, the filtered signal will be amplified to improve its amplitude, which significantly promotes the readiness of the signal identification. The amplified signal will then be converted from analog signal to digital signal by an AD converter, which makes the signal be processed by the sampling part in a more convenient, efficient and precise way. The original weak voltage signal will become recognizable after conducting through the signal process circuit. As presented in Fig. 4d and e, the peak signal voltage of the electrodes beneath the contact area reaches ~ 150 mV, which is much higher than the peak signal voltage of the noncontact area. After acquired and processed by a multi-channel system, the deduced result

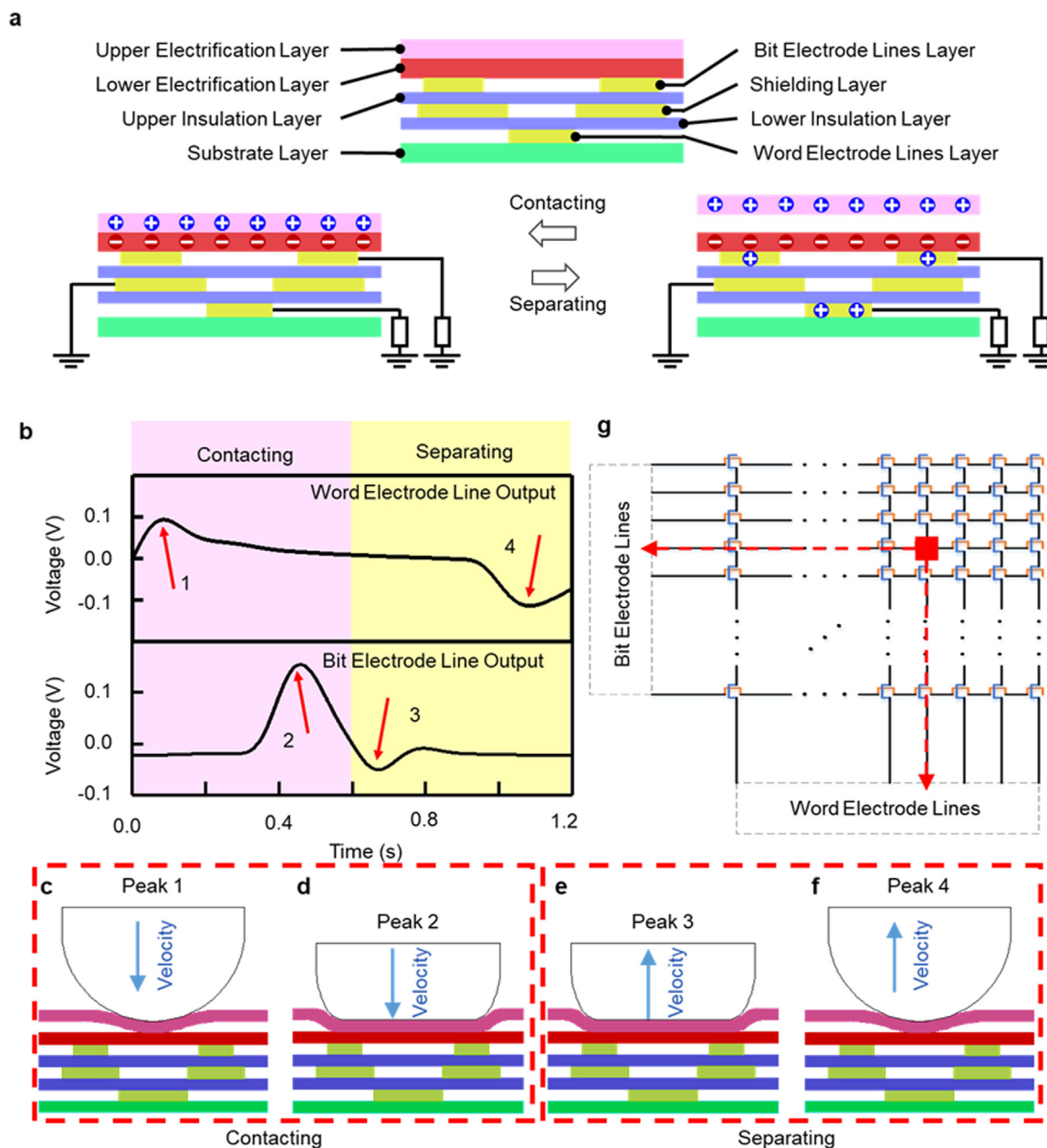


Fig. 2. Sensing principles of a single sensing unit and the sensing matrix. (a) Cross-sectional view of a single sensing unit and charge distribution illustration within a separating-contacting cycle. (b) Voltage output of the corresponding bit electrode line and word electrode line underneath the contacting unit in a separating-contacting cycle. (c), (d), (e) and (f) Illustration of the signal generation mechanism corresponding to peak 1, 2, 3 and 4 in (b), respectively. (g) Positioning principle of the ITESM.

can clearly reflect the shape profile of the contact object, as shown in Fig. 4f. It is worth of noting that no power source is supplied onto the ITESM. When the ITESM is in a stand-by mode without being touched, power is only needed to provide the very small silent current of the signal processing circuit. Wherefore, the energy consumption of the ITESM is exceptionally small even if a large number of sensing units are involved.

3. Experimental section

3.1. Fabrication of an ITESM

The ITESM was fabricated on a PI film (Kapton, DuPont) in a layer-by-layer process. The entire fabrication process consisted of six steps, which included sequential fabrication of the word electrode layer, the

lower insulation layer, the shielding layer, the upper insulation layer, the bit electrode layer and the lower electrification layer. As the substrate layer, the PI film was ultrasonically cleaned with acetone, isopropyl, alcohol and deionized water for 1 min, respectively. In order to facilitate photolithography, the PI film was affixed to a silicon wafer with the assistance of a photoresist (SUN-9i, 50 cP, SUNTIFIC Material (Weifang), LTD). A photoresist pattern of the word electrode lines was formed on the PI film by photolithography, and then 300 nm silver was deposited by e-beam evaporator method (E-BEAM EVAPORATOR, DENTON VACUUM). After removing the photoresist pattern, 3 μm Parylene C was deposited to construct the lower insulation layer by chemical vapor deposition method (PDS 2010, Special Coating System). Then, a photoresist pattern of the shielding layer was formed on the lower insulation layer by photolithography. Later that, a layer of 300 nm silver was deposited by e-beam evaporator method. Another

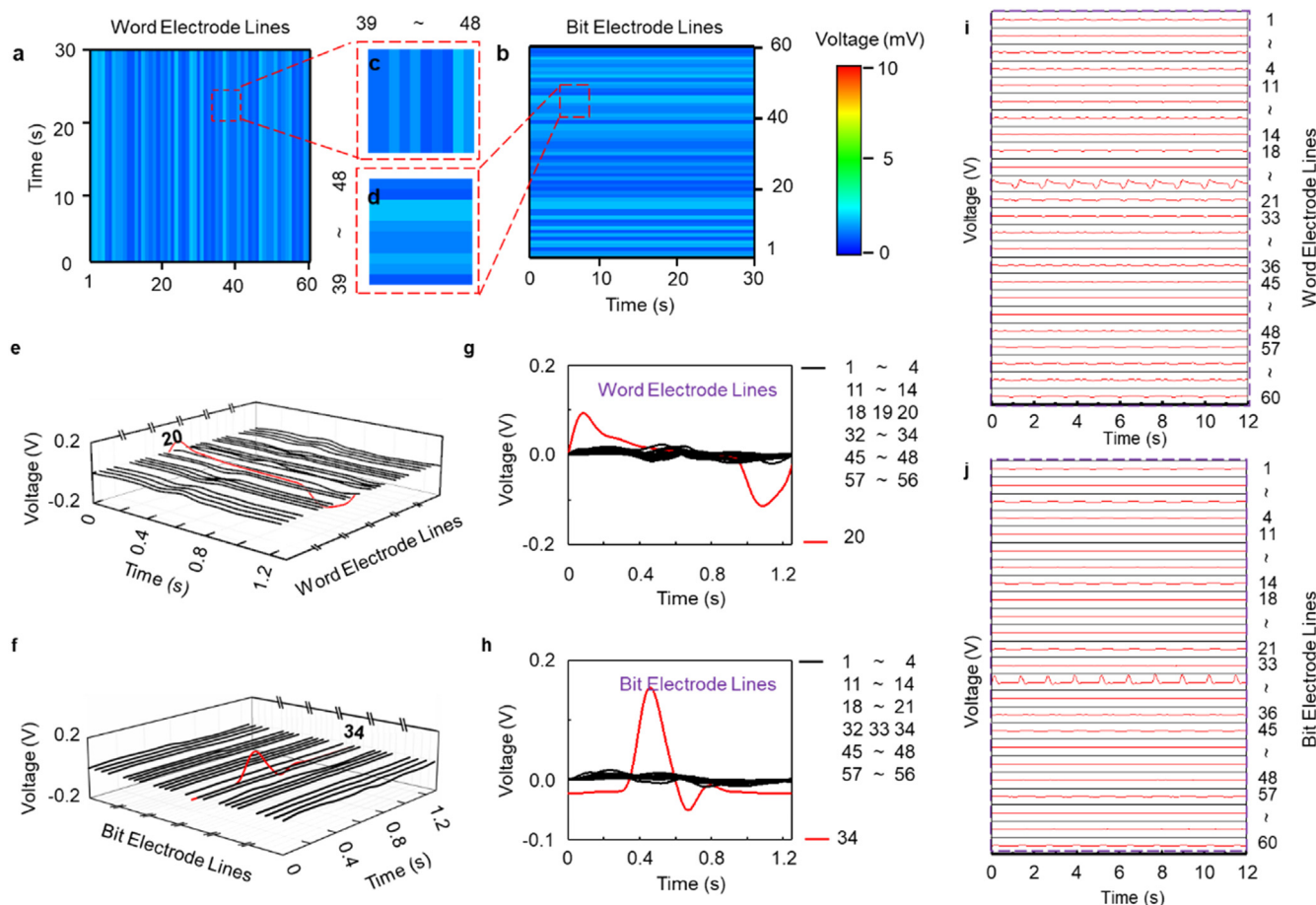


Fig. 3. Experimentally measured output voltage of the ITESM. The output voltage from the word electrode lines (a) and the bit electrode lines (b) without a contact, and the enlarged view of the output voltage from the selected word electrode lines (c) and bit electrode lines (d). Output voltage from 24 word electrodes lines (e) and 24 bit electrode lines (f) when a single unit is touched. (g) and (h) The lateral view of the output voltage corresponding to (e) and (f), respectively. Output voltage from the word electrode lines (i) and the bit electrode lines (j) in cyclic tests.

3 μm Parylene C film was deposited to construct the upper insulation layer once the photoresist pattern was removed. The last photoresist pattern of the bit electrode lines layer was formed on the upper insulation layer by photolithography. Finally, a layer of 3 μm Parylene C was deposited to form the lower electrification layer after the photoresist pattern was removed. The upper electrification layer of the ITESM was made of the TPU membrane. Firstly, a $6 \times 6 \text{ cm}^2$ frame with a hollow square size of $5 \times 5 \text{ cm}^2$ was made of acrylic by laser cutting (Pls.75–50, Universal laser system), and then a $6 \times 6 \text{ cm}^2$ TPU membrane was stretched and adhered onto the surface of the frame by a double-sided tape. A 5 mm thick sponge tapes was cut into four $5 \times 5 \text{ mm}^2$ solid squares and pasted on the four corners of the frame. The fabricated ITESM was affixed on a testing interface based on a printed circuit board. Each electrode line is connected to the testing interface for data acquisition. A hemispheric marker tip made of sponge was used as the contact object to excite a single sensing unit. The maximum diameter of the marker tip is about 550 μm .

3.2. Electric measurement

A surface electric potential meter (Model 279, MONROE Electronics) was used to measure the surface electric potential of the lower electrification layer. A multi-channel measurement system (PXIe 4300, National Instruments Corporation) was used to collect the electric signal that has been filtered and amplified. In signal processing circuit, a filtering chip (MAX7427, Maxim Integrated) was used to reduce the signal noise, and an amplification chip (MAX4465, Maxim Integrated)

was applied to achieve an amplification factor of 20.

4. Conclusion

The ITESM reported in this work has several unique features and merits. Foremost, the ITESM has an overall thickness of 20 μm , which is the thinnest triboelectric sensor array reported by far. It has an effective area of $3 \times 3 \text{ cm}^2$ that contains a total of 3600 sensing units, which reaches 400 dots per square centimeter and is 14 times than that of the state-of-the-art works on the triboelectric sensor array. The sensing resolution reaches 50 dpi, which poses a 25-times enhancement over the recently published works. A signal processing circuit is designed, which can effectively filters the environment noises and significantly amplifies the acquired signal. Attributed to the shielding layer and the signal processing circuit, the amplitude of the voltage signal reaches $\sim 0.4 \text{ V}$ from the electrode lines under the contacted point, while the maximum voltage signal from other electrode lines is only $\sim 0.02 \text{ V}$. The NEXT is calculated to be 0.05, which represents the readiness of signal recognition.

In summary, a thin-film-based flexible integrated triboelectric sensing matrix was developed. Based on the combination of triboelectrification effect and electrostatic induction, the ITESM produces a voltage output when contacted with an external object. The size of a single unit is $500 \times 500 \mu\text{m}^2$, which indicates the ITESM can acquire the image in a resolution as high as 50 dpi. Together with a measurement system, a sixty-by-sixty pixelated sensing matrix is demonstrated and used to distinguish the position and the contact shape profile. We

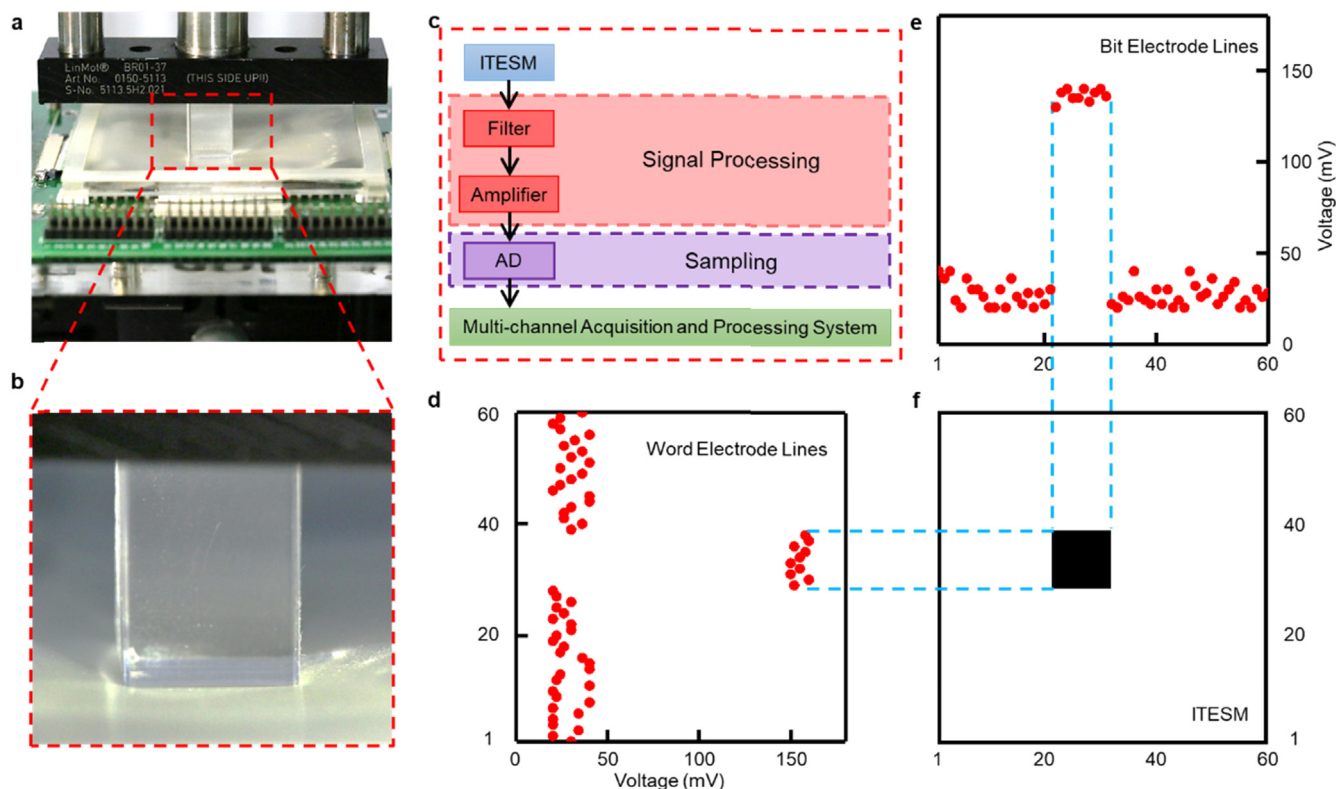


Fig. 4. Demonstration of the ITESM for imaging. (a) Photograph of the experimental setup for testing the ITESM. (b) An enlarged view of the contact object. (c) Process flow of the signal measurement system. The peak output voltage from all of the 60 word electrode lines (d) and the 60 bit electrode lines (e). (f) The remapped results of the shape profile and the position of the contact object.

believe this sensing matrix has significant potential for future development in human-machine interfacing technologies of electronic signature, fingerprint recognition, artificial skin and security monitoring.

Acknowledgements

This research was supported by the National Key R & D Project from Ministry of Science and Technology, China (Grant No. 2016YFA0202701 and 2016YFA0202703), National Science Foundation of China (Grant No. 51572030 and 51675069), Natural Science Foundation of Beijing Municipality (Grant No. 2162047) and China Thousand Talents Program.

References

- [1] J. Tegin, J. Wikander, *Ind. Robot.* 32 (2005) 64.
- [2] M.L. Hammock, A. Chortos, B.C. Tee, J.B. Tok, Z.N. Bao, *Adv. Mater.* 25 (2013) 5997.
- [3] A. Chortos, J. Liu, Z.N. Bao, *Nat. Mater.* 15 (2016) 937.
- [4] R.S. Dahiya, G. Metta, M. Valle, G. Sandini, *IEEE Trans. Robot.* 26 (2010) 1.
- [5] D.P.J. Cotton, P.H. Chappell, A. Cranny, N.M. White, S.P. Beeby, *IEEE Sens. J.* 7 (2007) 752.
- [6] M.H. Zhao, Z.L. Wang, S.X. Mao, *Nano Lett.* 4 (2004) 587.
- [7] W. Zhang, R.G. Xiong, *Chem. Rev.* 112 (2012) 1163.
- [8] T. Toriyama, S. Sugiyama, *J. Microelectromech. Syst.* 11 (2002) 598.
- [9] M.J. Jiang, Z.M. Dang, H.P. Xu, *Appl. Phys. Lett.* 90 (2007) 3.
- [10] J. Dargahi, S. Najarian, *Int. J. Med. Robot. Comput. Assist. Surg.* 1 (2004) 23.
- [11] C. Metzger, E. Fleisch, J. Meyer, M. Dansachmuller, I. Graz, M. Kaltenbrunner, C. Keplinger, R. Schwodiauer, S. Bauer, *Appl. Phys. Lett.* 92 (2008) 3.
- [12] D.J. Lipomi, M. Vosgueritchian, B.C.K. Tee, S.L. Hellstrom, J.A. Lee, C.H. Fox, Z.N. Bao, *Nat. Nanotechnol.* 6 (2011) 788.
- [13] J.A. Dobrzynska, M.A.M. Gijs, *J. Micromech. Microeng.* 23 (2013) 11.
- [14] C. Larson, B. Peele, S. Li, S. Robinson, M. Totaro, L. Beccai, B. Mazzolai, R. Shepherd, *Science* 351 (2016) 1071.
- [15] Q.L. Hua, H.T. Liu, J. Zhao, D.F. Peng, X.N. Yang, L. Gu, C.F. Pan, *Adv. Electron. Mater.* 2 (2016) 5.
- [16] Y.C. Lai, B.W. Ye, C.F. Lu, C.T. Chen, M.H. Jao, W.F. Su, W.Y. Hung, T.Y. Lin, Y.F. Chen, *Adv. Funct. Mater.* 26 (2016) 1286.
- [17] H.H. Chou, A. Nguyen, A. Chortos, J.W.F. To, C. Lu, J.G. Mei, T. Kurosawa, W.G. Bae, J.B.H. Tok, Z.N. Bao, *Nat. Commun.* 6 (2015) 10.
- [18] G. Zhu, W.Q. Yang, T. Zhang, Q. Jing, J. Chen, Y.S. Zhou, P. Bai, Z.L. Wang, *Nano Lett.* 14 (2014) 3208.
- [19] Y. Su, G. Zhu, W.Q. Yang, J. Yang, J. Chen, Q. Jing, Z.M. Wu, Y.D. Jiang, Z.L. Wang, *ACS Nano* 8 (2014) 3843.
- [20] X.Z. Jiang, Y.J. Sun, Z.Y. Fan, T.Y. Zhang, *ACS Nano* 10 (2016) 7696.
- [21] W.Q. Yang, J. Chen, X.N. Wen, Q.S. Jing, J. Yang, Y.J. Su, G. Zhu, W.Z. Wu, Z.L. Wang, *ACS Appl. Mater. Interfaces* 6 (2014) 7479.
- [22] F.R. Fan, Z.Q. Tian, Z.L. Wang, *Nano Energy* 1 (2012) 328.
- [23] F.R. Fan, L. Lin, G. Zhu, W.Z. Wu, R. Zhang, Z.L. Wang, *Nano Lett.* 12 (2012) 3109.
- [24] L. Lin, Y.N. Xie, S.H. Wang, W.Z. Wu, S.M. Niu, X.N. Wen, Z.L. Wang, *ACS Nano* 7 (2013) 8266.
- [25] X.D. Wang, H.L. Zhang, L. Dong, X. Han, W.M. Du, J.Y. Zhai, C.F. Pan, Z.L. Wang, *Adv. Mater.* 28 (2016) 2896.
- [26] X.X. Zhu, X.S. Meng, S.Y. Kuang, X.D. Wang, C.F. Pan, G. Zhu, Z.L. Wang, *Nano Energy* 41 (2017) 387.
- [27] J.C. Isaacs, N.A. Strakhov, *52*, 101, 1973.



Xiao Xiao Zhu received his bachelor's degree in Material Chemistry from Suzhou University of Science and Technology. Now he is pursuing his doctor's degree in Beijing Institute of Nanoenergy and Nanosystem, Chinese Academy of Sciences. His current research mainly focuses on flexible film sensing matrix based on triboelectric nanogenerators.



Ze Bin Li received his bachelor's degree in Thermal Energy and Power Engineering from Sichuan University. Now he is pursuing his master's degree in Beijing Institute of Nanoenergy and Nanosystem, Chinese Academy of Sciences. His current research mainly focused on energy harvesting devices based on triboelectric nanogenerators.



Bing Wu Su received his B.S. degree in Applied Physics from Taiyuan University of Technology in 2015 and M.Sc. degree in Materials Engineering and Nanotechnology from City University of Hong Kong in 2017. In May 2017, he became a graduate engineer trainee in Beijing Institute of Nanoenergy and Nanosystems, Chinese Academy of Sciences. His research focuses on fabrication of flexible nanodevices for force sensing and heavy metal ion detection.



Xiao Shi Li received the B.E. degree in electronic science and technology, and the M.E. degree in instrumentation engineering from Chongqing University, Chongqing, China, in 2014 and 2017, respectively. He is currently with the College of Optoelectronic Engineering, Chongqing University. His research interests include signal processing circuit, sensors and actuators, and instrumentation.



Dr. Jin Yang received the B.E., M.E. and Ph.D. degrees in instrumentation science and technology from Chongqing University in 2002, 2004, and 2007, respectively. Currently, he is a professor with the College of Optoelectronic Engineering, Chongqing University. His current research interests focus on sensor and actuator, measurement and instrumentation, nanogenerator, self-powered sensor and systems



Li Su is a postdoctoral research fellow at the Beijing Institute of Nanoenergy and Nanosystems, Chinese Academy of Sciences. She received her Ph.D. degree from Sun Yat-sen University in 2014, and her Bachelor degree from Guizhou University in 2008. Her current research interests include new energy materials and devices, force-light-electric coupling effect, and flexible sensors.



Prof. Zhong Lin Wang received his Ph.D. from Arizona State University in physics. He now is the Hightower Chair in Materials Science and Engineering, Regents' Professor, Engineering Distinguished Professor and Director, Center for Nanostructure Characterization, at Georgia Tech. Dr. Wang has made original and innovative contributions to the synthesis, discovery, characterization and understanding of fundamental physical properties of oxide nanobelts and nanowires, as well as applications of nanowires in energy sciences, electronics, optoelectronics and biological science. His discovery and breakthroughs in developing nanogenerators established the principle and technological road map for harvesting mechanical energy from environment and biological systems for powering personal electronics. His research on selfpowered nanosystems has inspired the worldwide effort in academia and industry for studying energy for micro-nano-systems, which is now a distinct disciplinary in energy research and future sensor networks. He coined and pioneered the field of piezotronics and piezophototronics by introducing piezoelectric potential gated charge transport process in fabricating new electronic and optoelectronic devices. Details can be found at: <http://www.nanoscience.gatech.edu>.



Dr. Xiao Yan Wei is an associate researcher at Shenzhen University. She received her Ph.D. degree in Condensed Matter Physics at Beijing Institute of Nanoenergy and Nanosystems, Chinese Academy of Sciences in 2018 and her Bachelor degree in Polymer Science and Engineering at Sichuan University in 2012. Her current research mainly focuses on efficient conversion of mechanical energy into light energy, which has widespread applications in the fields of energy harvesting, visual sensing, light source, display and so on.



Dr. Guang Zhu is a professor at Beijing Institute of Nanoenergy and Nanosystems, Chinese Academy of Sciences. He received his Ph.D. degree in Materials Science and Engineering at Georgia Tech in 2013 and his Bachelor degree in Materials Science and Engineering at Beijing University of Chemical Technology in 2008. His current research mainly focuses on designing, fabrication, and implementation of innovative miniaturized high-efficiency generators that harvest and convert ambient mechanical energy into electricity.



Shuang Yang Kuang received his bachelor's degree in Physics from Shandong University. Now he is pursuing his doctor's degree in Beijing Institute of Nanoenergy and Nanosystem, Chinese Academy of Sciences. His current research mainly focuses on application and fabrication of triboelectric nanogenerators.